Article

Supramolecular Isomerism, Framework Flexibility, Unsaturated Metal Center, and Porous Property of Ag(I)/Cu(I) 3,3‘,5,5‘-Tetrametyl-4,4‘-Bipyrazolate

Jie-Peng Zhang, and Susumu Kitagawa

J. Am. Chem. Soc., **2008**, 130 (3), 907-917 • DOI: 10.1021/ja075408b

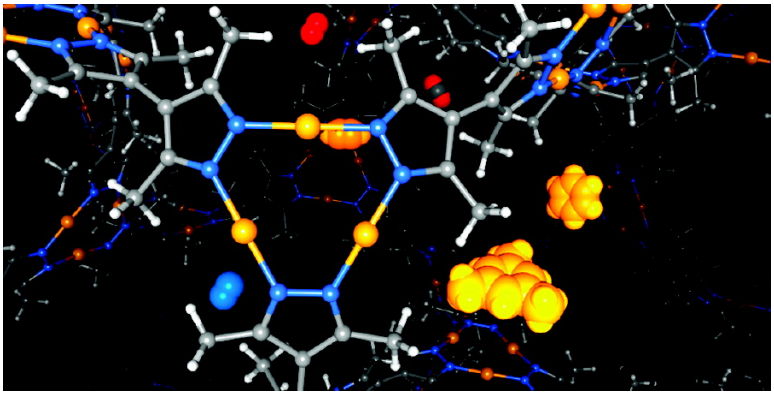

J|A|C|S
ARTICLES
Published on Web 01/01/2008

Supramolecular Isomerism, Framework Flexibility, Unsaturated Metal Center, and Porous Property of Ag(I)/Cu(I) 3,3′,5,5′-Tetrametyl-4,4′-Bipyrazolate

Jie-Peng Zhang† and Susumu Kitagawa*

Department of Synthetic Chemistry and Biological Chemistry, Graduate School of Engineering, Kyoto University, Katsura, Nishikyo-ku, Kyoto 615-8510, Japan

Received July 20, 2007; E-mail: kitagawa@sbchem.kyoto-u.ac.jp

Abstract: Template-controlled reactions of 3,3′,5,5′-tetramethyl-4,4′-bipyrazole (H_2bpz) with $[Ag(NH_3)_2]^+$ or $[Cu(NH_3)_2]^+$ give binary metal bipyrazolates [M_2(bpz)] (M = Ag, Cu) as two supramolecular isomers (**1** and **2**). Isomer **1** possesses four-fold interpenetrated (10,3)-*a* coordination networks, two-fold interpenetrated (10,3)-*a* channel networks, and guest-accessible coordinatively unsaturated metal clusters. Isomer **2** possesses eight-fold interpenetrated (6^2·10)(6·10^2) coordination networks and isolated, small pores. These metal bipyrazolates are chemically stable and thermally stable up to 300−500 °C. Their exceptional framework flexibilities have been demonstrated by adsorption measurements and single-crystal diffraction analyses. The guest-accessible Ag(I)/Cu(I) UMC clusters have also been demonstrated to facilitate the accommodation of unsaturated hydrocarbons such as benzene, toluene, mesitylene, and acetylene via weak metal···π interactions.

Introduction

The construction and characterization of porous coordination polymers (PCPs) have attracted much attention in recent years, and progress has been achieved in the aspects of stability, porosity, and pore shape/size regarding the application such as storage, separation, and catalysis.[1−8] However, the rational construction of PCP remains a great challenge for the difficulty in predicting the overall metal−organic connectivity or even the local coordination geometry.[2−6]

Due to the weak bonding between metal ions and organic ligands, coordination polymers usually collapse after guest removal and cannot show permanent porosity. Regarding this background, researchers have pursued the synthesis of highly porous and robust metal−organic frameworks by using rigid building blocks.[1−3,7,8] However, framework flexibility has been recognized as an advantage for high-performance molecular recognition, separation, and sensing applications.[1,4] In contrast to the rigid porous materials, a flexible PCP can expand, shrink, or distort its soft coordination network to fit the target molecules (Scheme 1).[9−17] In the case of a multiple interpenetrated PCP, pore deformation can also be derived from the internetwork

† Permanent address: School of Chemistry and Chemical Engineering, Sun Yat-Sen University, Guangzhou 510275, P.R. China.

(1) (a) Rosseinsky, M. J. *Microporous Mesoporous Mater.* **2004**, *73*, 15−30. (b) Kitagawa, S.; Kitaura, R.; Noro, S. I. *Angew. Chem., Int. Ed.* **2004**, *43*, 2334−2375. (c) Kepert, C. J. *Chem. Commun.* **2006**, 695−700.
(2) (a) Eddaoudi, M.; Moler, D. B.; Li, H.-L.; Chen, B.-L.; Reineke, T. M.; O'Keeffe, M.; Yaghi, O. M. *Acc. Chem. Res.* **2001**, *34*, 319−330. (b) Yaghi, O. M.; O'Keeffe, M.; Ockwig, N. W.; Chae, H. K.; Eddaoudi, M.; Kim, J. *Nature* **2003**, *423*, 705−714.
(3) Janiak, C. *Dalton Trans.* **2003**, 2781−2804.
(4) (a) Fletcher, A. J.; Thomas, K. M.; Rosseinsky, M. J. *J. Solid State Chem.* **2005**, *178*, 2491−2510. (b) Kitagawa, S.; Uemura, K. *Chem. Soc. Rev.* **2005**, *34*, 109−119.
(5) (a) Papaefstathiou, G. S.; MacGillivray, L. R. *Coord. Chem. Rev.* **2003**, *246*, 169−184. (b) Kitagawa, S.; Noro, S. I.; Nakamura, T. *Chem. Commun.* **2006**, 701−707.
(6) (a) Robson, R. *J. Chem. Soc., Dalton Trans.* **2000**, 3735−3744. (b) Moulton, B.; Zaworotko, M. J. *Chem. Rev.* **2001**, *101*, 1629−1658.
(7) Férey, G.; Mellot-Draznieks, C.; Serre, C.; Millange, F.; Dutour, J.; Surblé, Margiolaki, S. I. *Science* **2005**, *309*, 2040−2042.
(8) (a) Lin, X.; Blake, A. J.; Wilson, C.; Sun, X. Z.; Champness, N. R.; George, M. W.; Hubberstey, P.; Mokaya, R.; Schröder, M. *J. Am. Chem. Soc.* **2006**, *128*, 10745−10753. (b) Lin, X.; Jia, J.; Zhao, X.; Thomas, K. M.; Blake, A. J.; Walker, G. S.; Champness, N. R.; Hubberstey, P. Schröder, M. *Angew. Chem., Int. Ed.* **2006**, *45*, 7358−7364. (c) Ma, S.-Q.; Sun, D.-F.; Ambrogio, M.; Fillinger, J. A.; Parkin, S.; Zhou, H.-C. *J. Am. Chem. Soc.* **2007**, *129*, 1858−1859. (d) Liu, Y.-L.; Kravtsov, V. C.; Larsen, R. Eddaoudi, M. *Chem. Commun.* **2006**, 1488−1490.
(9) (a) Serre, C.; Mellot-Draznieks, C. Surblé, S.; Audebrand, N.; Filinchuk, Y.; Férey, G. *Science* **2007**, *315*, 1828−1831. (b) Matsuda, R.; Kitaura, R.; Kitagawa, S.; Kubota, Y.; Kobayashi, T. C.; Horike, S.; Takata, M. *J. Am. Chem. Soc.* **2004**, *126*, 14063−14070. (c) Serre, C.; Bourrelly, S.; Vimont, A.; Ramsahye, N. A.; Maurin, G.; Llewellyn, P. L.; Daturi, M.; Filinchuk, Y.; Leynaud, O.; Barnes, P.; Férey, G. *Adv. Mater.* **2007**, *19*, 2246−2251.
(10) (a) Dybtsev, D. N.; Chun, H.; Kim, K. *Angew. Chem., Int. Ed.* **2004**, *43*, 5033−5036. (b) Lee, E. Y.; Jang, S. Y.; Suh, M. P. *J. Am. Chem. Soc.* **2005**, *127*, 6374−6381. (c) Halder, G. J.; Kepert, C. J. *J. Am. Chem. Soc.* **2005**, *127*, 7891−7900.
(11) (a) Biradha, K.; Fujita, M. *Angew. Chem., Int. Ed.* **2002**, *41*, 3392−3395. (b) Biradha, K.; Hongo, Y.; Fujita, M. *Angew. Chem., Int. Ed.* **2002**, *41*, 3395−3398. (c) Wu, C.-D.; Lin, W.-B. *Angew. Chem., Int. Ed.* **2005**, *44*, 1958−1561. (d) Chen, B. L.; Liang, C. D.; Yang, J.; Contreras, D. S.; Clancy, Y. L.; Lobkovsky, E. B.; Yaghi, O. M.; Dai, S. *Angew. Chem., Int. Ed.* **2006**, *45*, 1390−1393.
(12) Takamizawa, S.; Nakata, E.-I.; Akatsuka, T. *Angew. Chem., Int. Ed.* **2006**, *45*, 2216−2221.
(13) Bradshaw, D.; Warren, J. E.; Rosseinsky, M. J. *Science* **2007**, *315*, 977−980.
(14) (a) Halder, G. J.; Kepert, C. J. *Aust. J. Chem.* **2006**, *59*, 597−604. (b) Suh, M. P.; Cheon, Y. E. *Aust. J. Chem.* **2006**, *59*, 605−612. (c) Vittal, J. J. C, *Coord. Chem. Rev.* **2007**, *251*, 1781−1795.
(15) Zhao, X.; Xiao, B.; Fletcher, A. J.; Thomas. K. M.; Bradshaw, D.; Rosseinsky, M. J. *Science* **2004**, *306*, 1012−1015.
(16) Pan, L.; Parker, B.; Huang, X.-Y.; Olson, D. L.; Lee, J. Y.; Li, J. *J. Am. Chem. Soc.* **2006**, *128*, 4180−4181.
(17) (a) Tanaka, D.; Masaoka, S.; Horike, S.; Furukawa, S.; Mizuno, M.; Endo, K.; Kitagawa, S. *Angew. Chem., Int. Ed.* **2006**, *45*, 4628−4631. (b) Shimomura, S.; Matsuda, R.; Tsujino, T.; Kawamura, T.; Kitagawa, S. *J. Am. Chem. Soc.* **2006**, *128*, 16416−16417. (c) Mulfort, K. L.; Hupp, J. T. *J. Am. Chem. Soc.* **2007**, *129*, 9604−9605.

Scheme 1

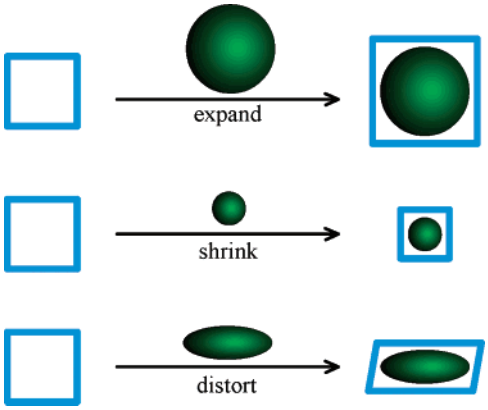

sliding. Such structural transformations are expected to occur uniformly throughout the whole coordination network as required by the extended cooperative effect of the crystal lattice. Therefore, the structural transformation of the host framework and the location of the guest molecule can be monitored by X-ray diffraction. Nevertheless, the stresses derived from the structural transformations tend to fracture the particles, especially the large ones. In general, strong bonding, high flexibility, and small structural change favor the so-called single-crystal-to-single-crystal transformations, which facilitate the precise structural determination by convenient single-crystal diffraction techniques. Besides the guest inclusion-induced structural transformations, the host frameworks of PCPs sometimes need to temporarily open their small apertures to allow the passage of large guest molecules, accompanying gate opening or hysteresis sorption behavior as a typical implication. Overall structural bistability is not necessary for this kind of framework flexibility; hence, the structure of the host framework may remain unchanged after guest inclusion.[15]

In addition to the framework flexibility, which offers close contact between the host framework and the guest molecule, PCPs also provide opportunity for direct pore surface engineering,[5] which is difficult for conventional porous materials such as inorganic zeolites and carbon molecular sieves. The pore surfaces of PCPs can be readily tailored by modification of the organic ligand with $\pi-\pi$ interaction, hydrogen bonding, and electron donor/acceptor functionalities.[16,17] Using coordinatively unsaturated metal centers (UMCs) represents a more intriguing strategy for pore surface modification, since transition metal ions can strongly interact with guest species. Although UMCs can also be introduced to inorganic porous materials, UMCs located inside PCPs take advantage from their uniform arrangements and well-understood surrounding environments. Studies of UMCs are mainly focused on the catalytic action, guest sensing, and hydrogen storage. Generating a UMC on the pore surface usually requires thermal liberation of the terminal ligand without destroying the host framework. Consequently, the most studied UMCs are based on "stable" coordination geometries, such as square planar Cu(II) and tetrahedral Zn(II), as well as some alkaline metal ions and lanthanide ions.[18−23]

The monovalent coinage metals Ag(I) and Cu(I) are attractive UMC candidates as soft Lewis acids. They can adopt diverse coordination geometries such as linear, trigonal planar, tetrahedral, etc. In the two- and three-coordinated forms, Ag(I)/Cu(I) retains large unoccupied space and is readily accessible for other soft Lewis base molecules. Ag(I)/Cu(I)-exchanged zeolites have shown high activities toward many important gases such as nitrogen, hydrogen, carbon monoxide, and unsaturated hydrocarbons.[24] Despite similar coordination behaviors, Ag(I) and Cu(I) UMCs can take different advantages from their different chemical/physical properties. For example, Ag(I) and Cu(I) are substantially different in electrochemical and photophysical properties. It should be noted that coordinatively unsaturated Cu(I) is a fundamental metal ion in the biological systems.[25] PCPs with guest-accessible Cu(I) centers may potentially serve as solid-state metalloenzyme mimics. Considering the density and price, copper is also more important than silver in a common sense. Nevertheless, immobilizing Ag(I)/Cu(I) UMC on the pore surface of a PCP is very difficult. First, Ag(I)/Cu(I) tends to have energetically stable tetrahedral coordination geometry rather than linear or trigonal planar ones. Second, Ag(I)/Cu(I) coordination complexes are very unstable and sensitive to light, heat, air, moisture, etc.

The concept of a binary metal azolate framework can be used to solve these problems.[26] Thanks to the strong metal azolate coordination bonds, binary metal azolate frameworks have demonstrated very high thermal stability and chemical stability.[27−30] More importantly, the coordination numbers of the monovalent metal centers are always equal to, or lower than, the numbers of nitrogen of the ligand, since each nitrogen donor can only coordinate to one metal center. For example, the coordination numbers of Ag(I)/Cu(I) are always two in the Ag(I)/Cu(I) imidazolates and pyrazolates. Nevertheless, simple Ag(I)/Cu(I) imidazolates and pyrazolates can only form discrete or chain-like, two-connected coordination structures. To construct a three-dimensional framework with two-coordinated metal centers, a tridentate or tetradentate ligand is necessary.

(18) Forster, P. M.; Eckert, J.; Chang, J.-S.; Park, S.-E.; Férey, G.; Cheetham, A. K. *J. Am. Chem. Soc.* **2003**, *125*, 1309−1312.
(19) Dietzel, P. D. C.; Panella, B.; Hirscher, M.; Bloma, R.; Fjellvåg, H. *Chem. Commun.* **2006**. 959−961. (b) Chen, B.; Ockwig, N. W.; Millward, A. R.; Contreras, D. S.; Yaghi, O. M. *Angew. Chem., Int. Ed.* **2005**, *44*, 4745−4749. (c) Dincă;, M.; Dailly, A.; Liu, Y.; Brown, C. M.; Neumann, D. A.; Long, J. R. *J. Am. Chem. Soc.* **2006**, *128*, 16876−16883. (d) Dincă;, M.; Han, W. S.; Liu, Y.; Dailly, A.; Brown, C. M.; Long, J. R. *Angew. Chem., Int. Ed.* **2007**, *46*, 1419−1422. (e) Peterson, P. K.; Liu, Y.; Brown, C. M.; Kepert, C. J. *J. Am. Chem. Soc.* **2006**, *128*, 15578−15579. (f) Ma, S.-Q.; Zhou, H.-C. *J. Am. Chem. Soc.* **2006**, *128*, 11734−11735. (g) Liu, Y.-L.; Eubank, J. F.; Cairns, A. J.; Eckert, J.; Kravtsov, V. C.; Luebke, R.; Eddaoudi, M. *Angew. Chem., Int. Ed.* **2007**, *46*, 3278−3283.
(20) Wu, C.-D.; Hu, A.-G.; Zhang, L.; Lin, W.-B. *J. Am. Chem. Soc.* **2005**, *127*, 8940−8941. (b) Cho, S.-H.; Ma, B.; Nguyen, S. T.; Hupp, J. T.; Albrecht-Schmitt, T. E. *Chem. Commun.* **2006**, 2563−2565.
(21) Horike, S.; Matsuda, R.; Tanaka, D.; Mizuno, M.; Endo, K.; Kitagawa, S. *J. Am. Chem. Soc.* **2006**, *128*, 4222−4223.
(22) Chen, B.; Yang, Y.; Zapata, F.; Lin, G.; Qian, G.; Lobkovsky, E. B. *Adv. Mater.* **2007**, *19*, 1693−1696.
(23) Cheng, X.-N.; Zhang, W.-X.; Lin, Y.-Y.; Zheng, Y.-Z.; Chen, X.-M. *Adv. Mater.* **2007**, *19*, 1494−1498.
(24) (a) Kargol, M.; Zajac, J.; Jones, D. J.; Steriotis, Th.; Rozière, J.; Vitse, P. *Chem. Mater.* **2004**, *16*, 3911−3918. (b) Serykh, A. I.; Kazansky, V. B. *Phys. Chem. Chem. Phys.* **2004**, *6*, 5250−5255. (c) Serykh, A. I.; Amiridis, M. D. *Microporous Mesoporous Mater.* **2006**, *94*, 320−324.
(25) (a) Prigge, S. T.; Eipper, B. A.; Mains, R. E.; Amzel, L. M. *Science* **2004**, *304*, 864−867. (b) Mirica, L. M.; Vance, M.; Rudd, D. J.; Hedman, B.; Hodgson, K. O.; Solomon, E. I.; Stack, T. D. P. *Science* **2005**, *308*, 1890−1892. (c) Himes, R. A.; Park, G. Y.; Barry, A. N.; Blackbum, N. J.; Karlin, K. D. *J. Am. Chem. Soc.* **2007**, *129*, 5352−5353.
(26) (a) Masciocchi, N.; Galli, S.; Sironi, A. *Comments Inorg. Chem.* **2005**, *26*, 1−37. (b) Zhang, J.-P.; Chen, X.-M. *Chem. Commun.* **2006**, 1689−1699.
(27) Liu, X.-Y.; Wang, Z.-G.; Lin, Y.-S.; Tang, L.-L.; Zhu, H.-L. *Synth. React. Inorg. Met.−Org. Chem.* **2005**, *35*, 155−159.
(28) Huang, X.-C.; Lin, Y.-Y.; Zhang, J.-P.; Chen, X.-M. *Angew. Chem., Int. Ed.* **2006**, *45*, 1557−1559.
(29) Park, K. S.; Ni, Z.; Côté, A. P.; Choi, J. Y.; Huang, R.; Uribe-Romo, F. J.; Chae, H. K.; O'Keeffe, M.; Yaghi, O. M. *Proc. Natl. Acad. Sci. U.S.A.* **2006**, *103*, 10186−10191.
(30) Tian, Y.-Q.; Zhao, Y.-M.; Chen, Z.-X.; Zhang, G.-N.; Weng, L.-H.; Zhao, D.-Y. *Chem. Eur. J.* **2007**, *13*, 4146−4154.

Scheme 2

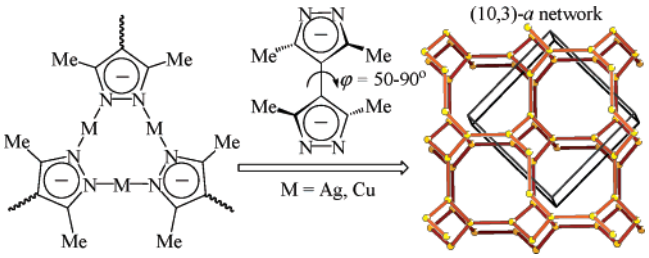

3,3′,5,5′-Tetramethyl-4,4′-bipyrazole (H_2bpz) has been extensively studied as a hydrogen-bonding synthon[31] and neutral bidentate ligand,[32] but deprotonated bpz has received less attention.[33,34] The coordination geometries of the coinage metal 3,3′,5,5′-tetramethyl-4,4′-bipyrazolate [M_2(bpz)] (M = Ag, Cu) can be readily predicted: each coinage metal ion should be coordinated by two nitrogen donors from two bpz ligands, and each bpz ligand is coordinated by four different metal ions. Because coinage metal 3,5-disubstituted pyrazolates frequently self-assembly as [M_3(pz)$_3$] triangles,[35,36] this robust motif can be expected as a targeted secondary building unit for [M_2(bpz)]. Considering that two 3,5-disubstituted pyrazolate moieties (pz) of bpz cannot be coplanar but reside at an dihedral angle between 50° and 90°, the default topology for [M_2(bpz)] should be a three-dimensional (3D) (10,3)-*a* net rather than a 2D (6,3) one (Scheme 2).[37]

Using this strategy, we have isolated a (10,3)-*a* network structure of [Ag_2(bpz)] and demonstrated the unusual framework flexibility of this framework material.[34] As an extension, we have successfully synthesized and structurally characterized the (10,3)-*a* network structure of [Cu_2(bpz)], which possesses not only large porosity but also guest accessible, two-coordinated Cu(I) centers unprecedented for PCPs. We also found that [M_2(bpz)] can crystallize as different structures at different conditions. Nevertheless, template-controlled supramolecular isomerism has been established for these metal bipyrazolates. The porous properties of these compounds are greatly influenced by the framework flexibility and UMC, which are further monitored by single-crystal diffraction studies.

Experimental Section

Materials and Physical Measurements. Commercially available reagents are used as received without further purification. 3,3′,5,5′-Tetramethyl-4,4′-bipyrazole (H_2bpz) is prepared by literature method.[32a] Thermal gravimetry (TG) was carried out with a Rigaku TG8120 in a nitrogen atmosphere except where indicated. X-ray powder diffraction (XRPD) data were collected on a Rigaku RINT-2200HF (Ultima) diffractometer with Cu Kα radiation. Gas adsorption isotherms were measured by using an Autosorb-1-C volumetric adsorption equipment from Quantachrome, U.S.A. Each point in the isotherms has an error less than ±0.15%, which is caused by the resolution of the pressure gauge.

Synthesis of α-[Ag_2(bpz)] (1-Ag). To a solution of Ag_2O (0.34 g, 2.0 mmol) dissolved in aqueous ammonia (28%, 20 mL), 150 mL of MeOH, and 5 mL of mesitylene was slowly added a solution of H_2bpz (0.38 g, 2.0 mmol) dissolved in MeOH (200 mL) with rigorous stirring at room temperature in ca. 1 day. The resultant white precipitate was solvent exchanged with MeOH (200 mL, 2 h with stirring, 6−8 times) until all mesitylene was removed. Finally, the solid was filtered and dried at reduced pressure to give a white powder (yield 450 mg, 55%). Single crystals of **1-Ag** can be obtained by layering a solution of H_2-bpz (20 mM) dissolved in EtOH (or MeCN) on a solution of Ag_2O (20 mM) dissolved in aqueous ammonia (28%). Colorless single crystals of **2-Ag** are also found in these diffusion reactions. The phase composition varies with different solvents and different batches.

α-[Cu_2(bpz)] (1-Cu). A mixture of Cu_2O (0.143 g, 1.0 mmol), aqueous ammonia (28%, 30 mL), MeOH (30 mL), toluene (2.0 mL), and H_2bpz (0.19 g, 1.0 mmol) was transferred into a 100-mL Teflon-lined autoclave and heated at 120 °C for 2 days. The resultant white precipitate was filtered, washed by MeOH, and dried at reduced pressure. Finally, toluene guest was removed by heating the white powder at 200 °C under vacuum (yield 240 mg, 75%). Heating the mixture at 150 °C for 10 days gave a few colorless single crystals with maximum dimension of ca. 0.1 mm. These single crystals were then heated at 200 °C under vacuum to remove the toluene and used for single-crystal X-ray diffraction studies.

***β*-[Ag_2(bpz)] (2-Ag).** To a solution of Ag_2O (0.34 g, 2.0 mmol) dissolved in aqueous ammonia (28%, 20 mL) and 150 mL MeOH was slowly added a solution of H_2bpz (0.38 g, 2.0 mmol) dissolved in MeOH (200 mL) with rigorous stirring at room temperature in ca. 1 day. The resultant white precipitate was filtered, washed by MeOH, and dried at reduced pressure. (yield 480 mg, 60%). Colorless single crystals can be obtained by layering a solution of H_2bpz (20 mM) dissolved in MeOH on a solution of Ag_2O (20 mM) dissolved in aqueous ammonia (28%)

***β*-[Cu_2(bpz)] (2-Cu).** A mixture of Cu_2O (0.143 g, 1.0 mmol), aqueous ammonia (28%, 10 mL), MeOH (30 mL), and H_2bpz (0.19 g, 1.0 mmol) was heated at 120 °C for 2 days. The resultant white precipitate was filtered, washed by MeOH, and dried at reduced pressure (yield 250 mg, 80%). Colorless single crystals can be obtained by heating the mixture at 150 °C for 4 days.

X-ray Crystallography. Diffraction intensities were collected on a Rigaku Mercury diffractometer (Mo Kα). Empirical absorption correction by using REQABA[38] was performed for all data. The structures were solved with direct methods and refined with a full-matrix least-squares technique with the SHELXTL program package.[39] For **1-Ag·I**, anisotropic thermal parameters were only applied to the metal atoms, and the bpz ligands were softly restrained to standard geometries. Although residual electron density can be found in the channel of **1-Ag·**

(31) (a) Boldog, I.; Rusanov, E. B.; Chernega, A. N.; Sieler, J.; Domasevitch, K. V. *Angew. Chem., Int. Ed.* **2001**, *40*, 3435−3438. (b) Boldog, I.; Rusanov, E. B.; Sieler, J.; Blaurockb, S.; Domasevitch, K. V. *Chem. Commun.* **2003**, 740−741.
(32) (a) Boldog, I.; Rusanov, E. B.; Chernega, A. N.; Sieler, J.; Domasevitch, K. V. *Polyhedron* **2001**, *20*, 887−897. (b) Ponomarova, V. V.; Komarchuk, V. V.; Boldog, I.; Chernega, A. N.; Sielerc, J.; Domasevitch, K. V. *Chem. Commun.* **2002**, 436−437. (c) Rusanov, E. B.; Ponomarova, V. V.; Komarchuk, V. V.; Stoeckli-Evans, H.; Fernandez-Ibanez, E.; Stoeckli, F.; Sieler, J.; Domasevitch, K. V. *Angew. Chem., Int. Ed.* **2003**, *42*, 2499−2501. (d) Domasevitch, K. V.; Boldog, I.; Rusanov, E. B.; Hunger, J.; Blaurock, S.; Schröder, M.; Sieler, J. *Z. Anorg. Allg. Chem.* **2005**, *631*, 1095−1100. (e) Ganesan, P. V.; Kepert, C. J. *Chem. Commun.* **2004**, 2168−2169.
(33) Crystal structure of an eight-fold interpenetrated ($6^2 \times 10$)(6×10^2) structure of [Cu_2(bpz)] is reported: He, J.; Yin, Y.-G.; Wu, T.; Li, D.; Huang, X.-C. *Chem. Commun.* **2006**, 2845−2847.
(34) Zhang, J.-P.; Horike, S.; Kitagawa, S. *Angew. Chem., Int. Ed.* **2007**, *46*, 889−892.
(35) (a) Kishimura, A.; Yamashita, T.; Aida, T. *J. Am. Chem. Soc.* **2005**, *127*, 179−183. (b) Yang, G.; Raptis, R. G. *Inorg. Chem.* **2003**, *42*, 261−263. (c) Dias, H. V. R.; Diyabalanage, H. V. K.; Eldabaja, M. G.; Elbjeirami, O.; Rawashdeh-Omary, M. A.; Omary, M. A. *J. Am. Chem. Soc.* **2005**, *127*, 7489−7501. (d) Omary, M. A.; Rawashdeh-Omary, M. A.; Gonser, M. W. A.; Elbjeirami, O.; Grimes, T.; Cundari, T. R. *Inorg. Chem.* **2005**, *44*, 8200−8210. (e) Dias, H. V. R.; Gamage, C. S. P. *Angew. Chem., Int. Ed.* **2007**, *46*, 2192−2194.
(36) (a) Hayashi, A.; Olmstead, M. M.; Attar, S.; Balch, A. L. *J. Am. Chem. Soc.* **2002**, *124*, 5791−5795. (b) Burress, C.; Elbjeirami, O.; Omary, M. A.; Gabbaï, F. P. *J. Am. Chem. Soc.* **2005**, *127*, 12166−12167.
(37) (a) Wells, A. F. *Three-Dimensional Nets and Polyhedra*; Wiley: New York, 1977. (b) Batten, S. R.; Robson, R. *Angew. Chem., Int. Ed.* **1998**, *37*, 1461−1494. (c) Carlucci, L.; Ciani, G.; Proserpio, D. M. *Coord. Chem. Rev.* **2003**, *246*, 247−289.
(38) Jacobson, R. A. *REQABA Empirical Absorption Correction*, version 1.1-0301998; Molecular Structure Corp.: The Woodlands, TX, 1996−1998.
(39) Sheldrick, G. M. *SHELXTL 6.10*; Bruker AXS Inc.: Madison, Wisconsin, 2000.

Table 1. Crystallographic Data and Structure Refinements

cmpd	1-Ag[34]	1-Ag–I	1-Ag·M	1-Cu	2-Ag	2-Cu
formula	$C_{10}H_{12}Ag_2N_4$	$C_{90}H_{108}Ag_{18}N_{36}$	$C_{222}H_{276}Ag_{30}N_{60}$	$C_{10}H_{12}Cu_2N_4$	$C_{60}H_{72}Ag_{12}N_{24}$	$C_{60}H_{72}Cu_{12}N_{24}$
FW	403.98	3635.78	7021.13	315.32	2423.86	1891.90
space group	$I\bar{4}3d$	$I\bar{4}2d$	$I41/a$	$I\bar{4}3d$	$Ccca$	$Ccca$
a/Å	27.2326(15)	27.1756(8)	61.7239(11)	26.407(3)	19.2056(5)	18.537(2)
b/Å					47.9669(16)	46.211(5)
c/Å		81.019(3)	26.9189(5)		36.2063(9)	34.925(4)
V/Å^3	20196.1(19)	59833(3)	102557(3)	18415(4)	33354.4(16)	29917(5)
Z	48	16	16	48	16	16
D_c/g cm^{-3}	1.594	1.614	1.819	1.365	1.931	1.680
T/K	213(2)	123(2)	153(2)	293(2)	213(2)	123(2)
μ/mm^{-1}	2.310	2.340	2.289	2.753	2.798	3.389
R1 ($I > 2\sigma$)[a]	0.0613	0.1664	0.0548	0.0642	0.0494	0.0512
wR2 (all data)[a]	0.1012	0.3870	0.1158	0.2063	0.0975	0.1109
GOF	1.010	1.437	1.051	1.013	1.014	1.029

[a] $R1 = \Sigma||F_o| - |F_c||/\Sigma|F_o|$, $wR2 = [\Sigma w(F_o^2 - F_c^2)^2/\Sigma w(F_o^2)^2]^{1/2}$.

I, they are not involved in the structure refinement due to the low diffraction data quality and the disorder of guest molecules. For other compounds, anisotropic thermal parameters were applied to all non-hydrogen atoms. The organic hydrogen atoms were generated geometrically. Crystal data as well as details of data collection and refinements for the complexes are summarized in Table 1.

Results and Discussion

Crystal Structures. The binary coinage metal bipyrazolates [M_2(bpz)] (M = Ag or Cu, bpz = 3,3′,5,5′-tetramethyl-4,4′-bipyrazolate) crystallize in two structural types α-[M_2bpz] (**1**) and β-[M_2bpz] (**2**).[6] The local coordination geometries of the two isomers are virtually identical as predicted and only slightly vary at the bond distances and angles. The Ag/Cu ions are linearly coordinated by two nitrogen donors from two bpz ligands, and each bpz ligand is coordinated to four Ag/Cu ions. The secondary structural motifs of these isomers are also identical. Three Ag/Cu ions are bridged by three pyrazolate moieties to form a triangle $M_3(pz)_3$, which is frequently observed in coinage metal pyrazolates,[35] pyridinates, and amidinates, etc.[36] Since two pyrazolate moieties of the bpz ligand are connected by a C−C single bond, the resultant [M_2(bpz)] coordination framework is polymeric. Nevertheless, the overall 3D structures of isomers **1** and **2** are different in the network topologies, interpenetration numbers, and pore structures.

α-[M_2(bpz)]. The M_2(bpz) coordination network of **1** can be simplified as a uniform (10,3)-*a* topology by considering the $M_3(pz)_3$ SBUs as three-connected nodes and the bpz ligands as linkers (Figure 1). The (10,3)-*a* topology, having the highest symmetry among all three-connected topologies, is expected as the default topology for the M_2(bpz) system, as $M_3(pz)_3$ SBU and the rotation angle of bpz ligand fully match the geometry requirement of (10,3)-*a* topology. Compared to the ideal (10,3)-*a* topology, the M_2(bpz) coordination networks of **1** are highly distorted. This distortion should mainly arise from the rotation of bpz ligands, as the ideal (10,3)-*a* topology possesses a 70.5° dihedral angle between adjacent trigonal nodes, while the dihedral angles of the bpz ligands are 67.4° and 63.4° in **1-Ag** and **1-Cu**, respectively. Nevertheless, the distortion of the $M_3(pz)_3$ SBUs from the ideal trigonal planar geometry also contributes the overall network distortion. Distorting from the highest symmetry always results in the contraction of volume. Using a node-to-node distance of 11.0 Å as determined in the crystal structure of **1-Ag**, a nondistorted [Ag_2(bpz)] network requires a cell volume of ca. 30,000 Å^3, 50% higher than the

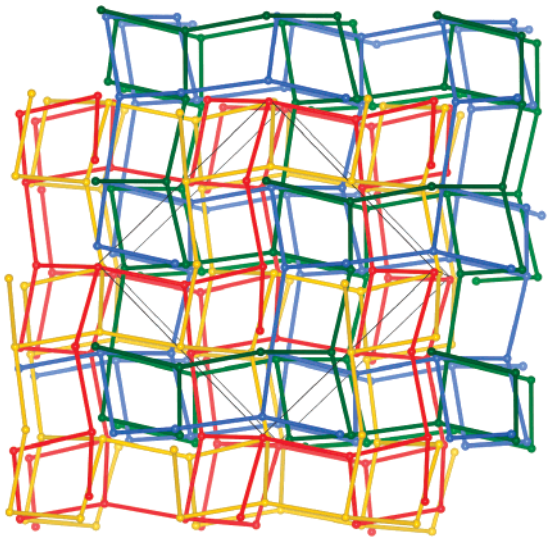

Figure 1. Four-fold interpenetrated (10,3)-*a* coordination networks of **1-Cu** (ball: Cu_3, triangle, stick: bpz ligand).

that of the distorted one in **1-Ag**. Nevertheless, a single distorted M_2(bpz) coordination network still occupies a very small fraction of the crystal volume. Actually, the whole 3D structure of **1** consists of two pairs of racemic (10,3)-*a* networks (Figure 1),[37] and retains about 30.3% and 33.7% voids for α-[Ag_2(bpz)] (**1-Ag**) and α-[Cu_2(bpz)] (**1-Cu**), respectively.[40] The M_2(bpz) networks are interlocked by face-to-face, staggered, metallophilic stacking between two $M_3(pz)_3$ SBUs of two adjacent nets. One of the two triangular $M_3(pz)_3$ faces remains unoccupied, leaving the M_3 triangles as UMCs. Interestingly, the extra frameworks in **1** are divided into two intersecting channels having a pair of racemic (10,3)-*a* topologies, in which the three-connected nodes are defined by the void space located between two $M_3(pz)_3$ SBUs or sandwiched by two M_3 UMC clusters, and the three-connected nodes are interconnected by small apertures ($d \approx 3.4$ Å) (Figure 2).

***β*-[M_2(bpz)].** Although the crystallography asymmetric unit of **2** contains 12 metal ions and 6 bpz ligands, the coordination network of **2** can be described as a binodal three-connected topology (6^2·10)(6·10^2) by using the same simplification rule as that for **1**. A single (6^2·10)(6·10^2) M_2(bpz) network of **2** is even more porous than that of **1**, allowing the eight-fold interpenetration (Figure 3). Actually, **2** contain only ca. 11%

(40) Spek, A. L. *PLATON*; Utrecht University: Utrecht, The Netherlands, 2003.

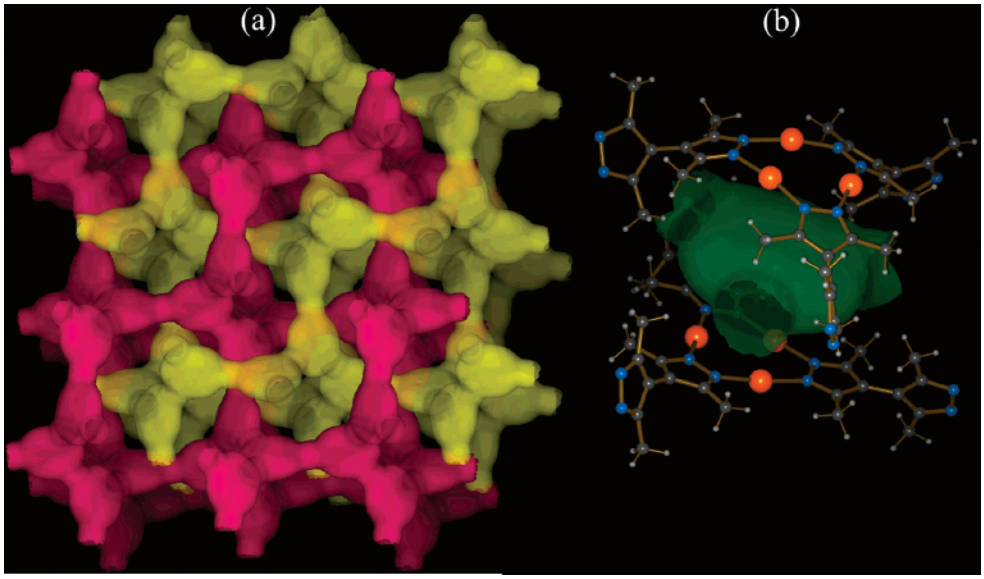

Figure 2. Two-fold interpenetrated channels (a) and the local pore environment (b) of **1-Cu**.

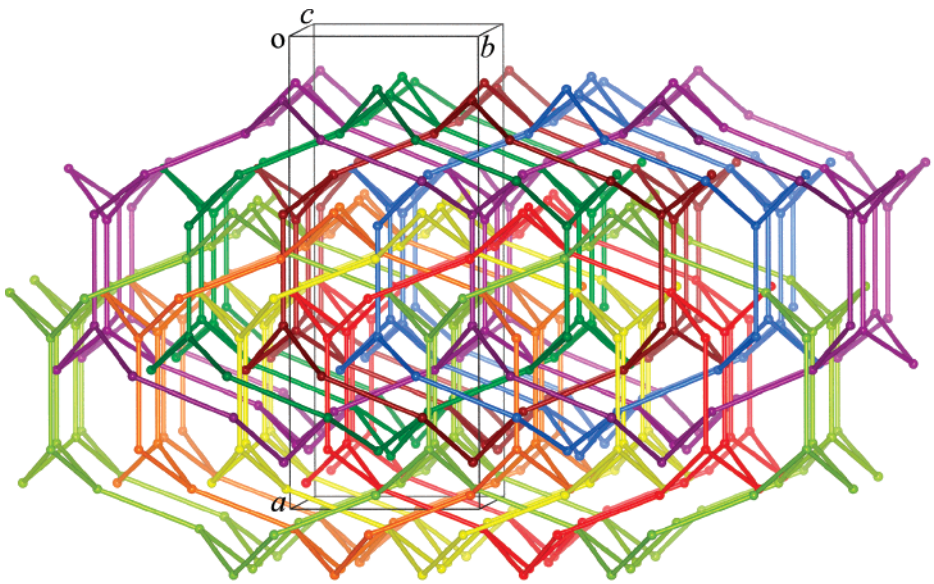

Figure 3. Eight-fold interpenetrated coordination networks of **2-Ag** (ball: Ag_3, triangle, stick: bpz ligand).

extra frameworks, and the small cavities are virtually isolated from each other since they are only interconnected by very small apertures with diameter less than 2 Å (see Supporting Information). The net-to-net contact of **2** is very different to that of **1**. Few $M_3(pz)_3$ SBUs form face-to-face, offset, metallophilic stacking dimers, while the others form infinite, face-to-face, offset, metallophilic stacking dimers (Figure 4). Therefore, the pore surfaces of **2** are mainly constituted by methyl groups of the bpz ligands; meanwhile, only a small fraction of the pore surfaces is in contact with the M_3 triangles.

Syntheses and Supramolecular Isomerism. Similar to other binary metal azolates, the $[M_2(bpz)]$ system is also highly insoluble. Preliminary crystallization trials showed that single crystals of **1-Ag** can be obtained by liquid diffusion between $[Ag(NH_3)_2]^+$ and H_2bpz in ethanol.[34] However, repeated experiments revealed that the reproducibility of this reaction is poor, as sometimes the final products also contain more or less **2-Ag** crystals. This phenomenon is termed concomitant polymorphism, which is fundamental to the understanding of the

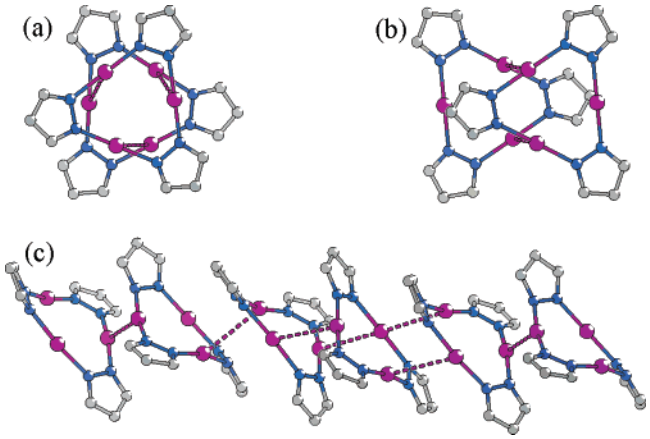

Figure 4. $[Ag_3(pz)_3]$ stacking modes of **1-Ag** (a), and **2-Ag** (b and c).

crystallization processes of organic and metal-organic systems. Actually, the $[M_2(bpz)]$ coordination networks can be viewed as the hydrogen-bonding network analogues of the H_2bpz ligand

Table 2. Crystallization Behavior of $[M_2(bpz)]$

		benzene or toluene	mesitylene	no template
Ag	rapid mixing	mixture/unidentified	**1** powder	**2** powder
	slow diffusion	mixture/unidentified	**1** crystal	**2** and **1** crystal
Cu	rapid mixing	**1** powder	**1** powder	**2** powder
	slow diffusion	**2** crystal	**2** crystal	**2** crystal

itself by considering the structural similarity of N−M−N coordination bonds and N−H···N hydrogen bonds. H_2bpz ligands do form multiple framework solids in different solvents, and one of them resembles the structure of **1**.

Controlling the crystallization of a supramolecular isomerism system is an important step toward the understanding of crystal engineering. Considering that the UMC cluster-functionalized pores of **1-Ag** are suitable to accommodate small arene molecules, we have tested the template effect of benzene, toluene, and mesitylene in the crystallization process of **1-Ag**. In the presence of mesitylene, $[M_2(bpz)]$ can be selectively crystallized as **1-Ag·mesitylene** in both slow-diffusion and rapid-mixing reactions. Benzene and toluene have weak template effects toward **1-Ag**. Concomitant polymorphism or structurally unidentified powder samples are observed when benzene and toluene are used as templates. Finally, **2-Ag** can be obtained as a pure phase in the absence of arene molecules.

The reaction of $[Cu(NH_3)_2]^+$ and bpz^{2-} tend to precipitate as powder rather than as a large, single crystal, since the solubility of $[Cu_2(bpz)]$ in common solvents and aqueous ammonia is even lower than that of $[Ag_2(bpz)]$. Probably because of the smaller cavity size of **1-Cu**, not only mesitylene but also benzene and toluene can template the rapid-mixing crystallization of **1-Cu·arene** powder samples. Hydrothermal treatment of these reaction mixtures can increase the crystal size of **1-Cu·arene**. However, the synthesis of a **1-Cu·arene** or **1-Cu** single crystal large enough for X-ray diffraction analysis is extremely difficult. A few single crystals of **1-Cu·toluene** with maximum diameter of ca. 0.1 mm can be obtained by hydrothermal treatment at 150 °C for two weeks. On the other hand, **1-Cu·benzene** transforms to **2-Cu** at the same reaction conditions. Surprisingly, in slow-diffusion experiments, all templates mentioned above give rise to the formation of **2-Cu** single crystals rather than the **1-Cu·arene** ones. Nevertheless, in the absence of template, **2-Cu** powder or single crystal is formed at rapid mixing or slow diffusion reactions, respectively.

The thermodynamic potential of $[M_2(bpz)]$ isomers can be tuned by the addition of an arene template. From benzene, toluene, to mesitylene, the larger molecule has the higher ability to stabilize the four-fold interpenetrated (10,3)-*a* network phase **1**. The remarkable difference of crystallization behavior between the rapid-mixing and slow-diffusion methods implies the importance of kinetic factors. As rapid mixing provides a homogeneous reaction environment for crystallization, the thermodynamically favored isomer can be obtained in a single phase. On the other hand, slow diffusion provides a heterogeneous reaction environment, and two isomers can start to crystallize at different regions. The crystal growing/recrystallization speed of **2-Cu** should be much higher than that of **1-Cu·arene**; hence, only **2-Cu** single crystals can be observed even in the presence of strong templates. As summarized in Table 2, the $[M_2(bpz)]$ supramolecular isomers and their molecular building blocks have delicately thermodynamic and dynamic balance, and $[Cu_2(bpz)]$ has a higher tendency than $[Ag_2(bpz)]$ to form phase **2**.

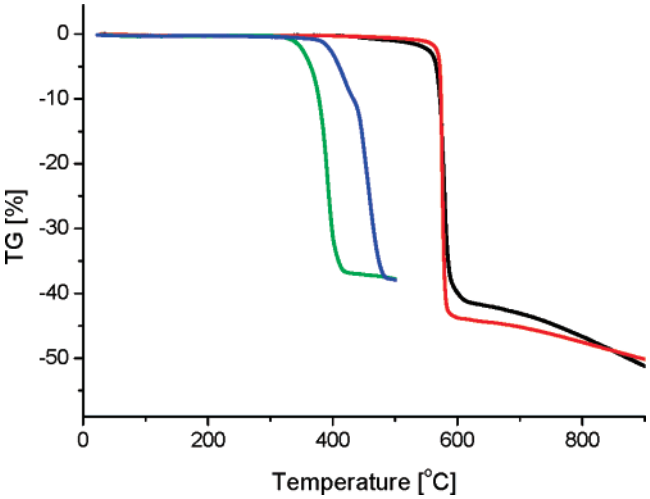

Figure 5. TG curves of **1-Ag** (green), **1-Cu** (black), **2-Ag** (blue), and **2-Cu** (red).

Framework Stability. No color change is evident while $[Ag_2(bpz)]$ isomers are exposed to ambient light for two weeks. The microcrystalline powder samples of **1-Cu** can be handled in air for short time, and its color changes from white to light green after 2 days, reflecting the oxidation of Cu(I) ions in air. However, after 1 month of exposure, the XRD pattern of the light-green powder still resembles that of **1-Cu**, although peak broadening and intensity decreasing are observed. The stability of **2-Cu** toward air and moisture are even higher, which can be ascribed to its nonporous structure.

The thermal stability of **1** and **2** are estimated by thermogravimetric (TG) and XRD diffraction measurements. The $[Ag_2(bpz)]$ isomers **1-Ag** and **2-Ag** decompose above 300 °C and 350 °C, respectively, which are higher than those of other Ag(I) coordination polymers. In nitrogen atmosphere, the $[Cu_2(bpz)]$ isomers are stable up to 500 °C (Figure 5), which is comparable to those of the most thermally stable MOFs. Nevertheless, in the air atmosphere, they start to decompose above 400 °C (see Supporting Information).[33]

The stability of these coinage metal bipyrazolates are remarkable since Ag(I)/Cu(I) coordination complexes are very unstable and sensitive to light, heat, moisture, air, etc. The highly interpenetrated framework structure and strong metal−pyrazolate coordination bonds should be responsible. Mutually interlocked coordination frameworks have been shown to increase thermal stability of MOFs. Compared to common nitrogen donors such as amine and pyridine, azole coordinates more strongly to transition metal ions because of the combination of strong basicity and π-accepting character. After deprotonation, the coordination ability of the resultant azolate ligand further increases from the gain of negative charge and higher basicity. Many binary metal azolates have been reported to have very high thermal stability and chemical stability.

Porosity and Framework Flexibility. From a static point of view, the small window opening ($d \approx 3.4$ Å) of **1** can only allow the adsorption of very small molecules, while the isolated pores of **2** are not accessible to the guest molecules. Gas adsorption isotherms of **1** and **2** were measured by using nitrogen, carbon dioxide, or oxygen. The kinetic diameters of

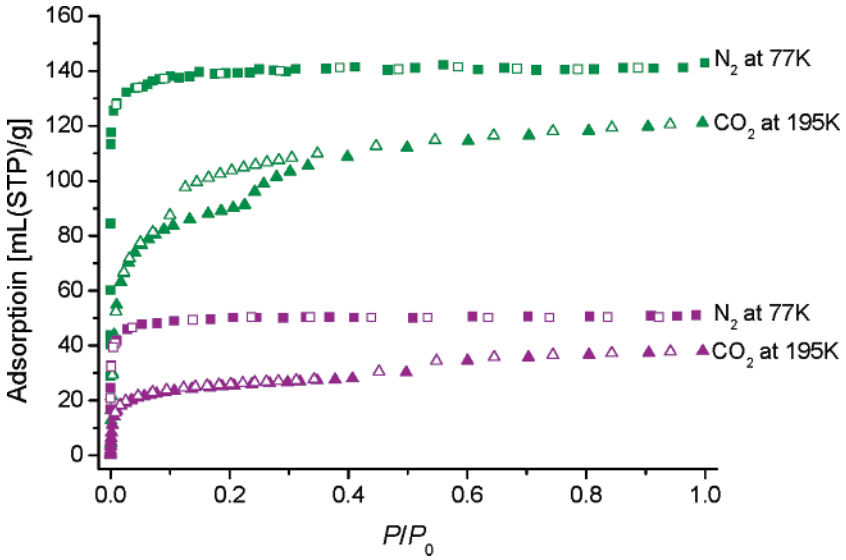

Figure 6. Nitrogen and carbon dioxide adsorption (solid) and desorption (open) isotherms of **1-Ag** (green) and **2-Ag** (purple).

nitrogen, oxygen, and carbon dioxide are 3.6, 3.46, and 3.3 Å, respectively.

Compound **1-Ag** showed a typical type-I nitrogen adsorption isotherm, having an apparent Langmuir surface area of 600 m^2/g and a pore volume of 0.218 mL/g. Assuming the crystal structure does not change during adsorption process, the pore volume of **1-Ag** is calculated to be only 0.188 mL/g. The excess adsorption of nitrogen implies that the host framework of **1-Ag** undergoes structural transformation during the adsorption process. However, no obvious multistep feature is found in the nitrogen adsorption, implying that the host framework of **1-Ag** may transform continuously and smoothly in a wide region of guest pressure.

The CO_2 isotherms of **1-Ag** revealed two consecutive adsorption/desorption steps and a hysteresis. The apparent Langmuir surface areas of the low and the high P/P_0 regions are about 540 and 720 m^2/g, respectively. The sudden increase of the surface area demonstrates the large difference of host structure at the two steps.[9] However, a continuous structural transformation cannot be ruled out for the low P/P_0 region since the surface area is still larger than expected.

Similar N_2 and CO_2 adsorption/desorption isotherms are also observed for **2-Ag**. Regarding that the aperture size of **2-Ag** is smaller than 2 Å, the abrupt increase of N_2 isotherm at very low P/P_0 unambiguously demonstrates the framework flexibility. Moreover, as in the case of **1-Ag**, the measured pore volume (N_2, 0.079 mL/g) of **2-Ag** is also much higher than the calculated one (0.056 mL/g). Similar to the CO_2 adsorption isotherm of **1-Ag**, a sudden phase transition also occurs for **2-Ag** (Figure 6).

Compound **1-Cu** also has a type-I N_2 sorption isotherm similar to that of **1-Ag**. Although the measured pore volume (0.250 mL/g) is only slightly larger than the calculated value (0.247 mL/g), a structural transformation should be taken into consideration, since the measured pore volumes of rigid PCPs are usually significantly lower than the calculated ones. Nevertheless, the extent of this structural transformation should be smaller than that of **1-Ag**. In contrast to **1-Ag**, only a one-step uptake was revealed from the CO_2 isotherm of **1-Cu**. Interestingly, the CO_2 isotherm of **1-Cu** resembles that of **1-Ag** at the low P/P_0 region. Therefore, the sudden structural transformation of **1-Ag**, induced by CO_2 at $P/P_0 = 0.22$, does not occur in the case of **1-Cu**.

Different to the above-mentioned compounds, **2-Cu** cannot adsorb N_2 at 77 K, but readily adsorbs O_2 at the same temperature. Because the pore aperture of **2-Cu** is significantly smaller than the kinetic diameters of N_2 (3.6 Å) and O_2 (3.4 Å), it can be concluded that the host framework is flexible but not flexible enough for N_2 molecules. Similar to other rigid PCPs, the measured pore volume of **2-Cu** lower than the value calculated from its crystal structure. The adsorption of CO_2 also demonstrates the framework flexibility, but the absence of sudden structural transformation indicates that **2-Cu** is not as flexible as the Ag(I) compounds (Figure 7).

The gas sorption behaviors of $[M_2(bpz)]$ show a clear tendency in the extent of framework flexibility, i.e., **1** > **2** and Ag > Cu (Table 3). The higher flexibility of isomer **1** should be attributed to the lower interpenetration number and larger free space. Moreover, isomer **1** possesses an uncommon internetwork metallophilic interaction conformation between the $M_3(pz)_3$ SBUs, which may easily transform to the energetically stable one as observed in the isomer **2** and other related compounds. The lower flexibility of $[Cu_2(bpz)]$ isomers can be explained by their shorter and stronger metal−nitrogen coordination bonds, which make the coordination network stiffer.

Besides small gas molecules, the highly flexible frameworks of isomer **1** also allow the reversible uptake/release of larger molecules, such as benzene (smallest cross section: 3.3 Å × 6.6 Å), toluene (4.0 Å × 6.6 Å), and mesitylene (4.1 Å × 8.2 Å).[41] Considering the cavity shape and pore surface, the arene molecules should be sandwiched by the M_3 triangles in a face-to-face fashion. Obviously, the M_3 triangle separations (**1-Ag** 8.9 Å, **1-Cu** 8.4 Å) are too large for one benzene ring but too small for two. Theoretically, a rigid host framework can accommodate only one benzene ring in each pore, and the remaining space is not utilizable. In the case of flexible host frameworks, the pores would either shrink to fit one benzene ring or expand for two or more benzene rings. Remarkably,

(41) Webster, C. E.; Drago, R. S.; Zerner, M. C. *J. Am. Chem. Soc.* **1998**, *120*, 5509−5516.

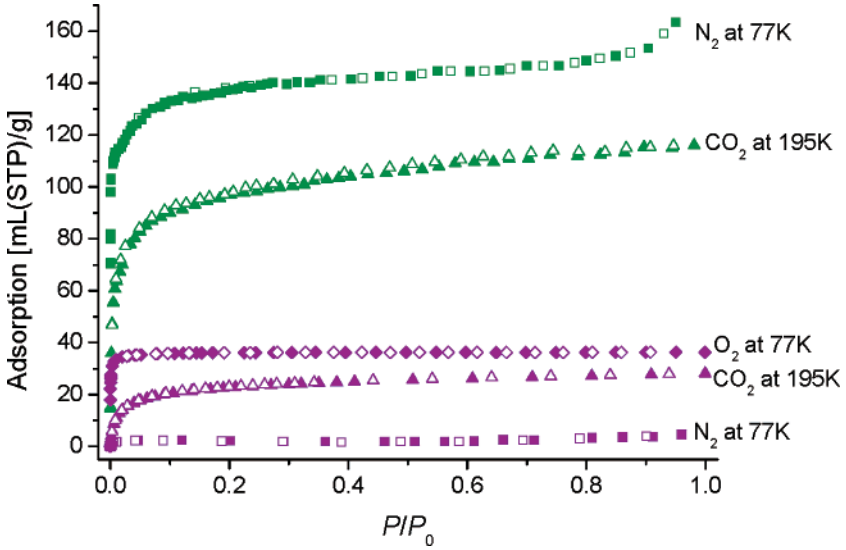

Figure 7. Nitrogen, carbon dioxide, and oxygen adsorption (solid) and desorption (open) isotherms of **1-Cu** (green) and **2-Cu** (purple).

Table 3. Porous Parameters of $[M_2(bpz)]$

	apparent surface area[a] [m²/g]	pore volume[c] [mL/g]	void[d] (%)	pore volume[e] [mL/g]
1-Ag	600	0.218	30.3	0.188
1-Cu	660	0.250	33.7	0.247
2-Ag	220	0.079	10.9	0.056
2-Cu	140[b]	0.045[b]	10.7	0.064

[a] Calculated from N_2 adsorption isotherms using Langmuir model except where indicated. [b] Oxygen as adsorbate. [c] Calculated from N_2 adsorption isotherms using Dubinin−Radushkevich equation except where indicated. [d] Calculated from crystal structures by PLATON. [e] Calculated from void percentage and crystal density.

single crystals of **1** retain single crystallinity during these uptake/release processes, providing direct structural evidence of the structural transformations. Single-crystal X-ray analyses of **1-Ag** fully loaded with benzene (**1-Ag·B**), toluene (**1-Ag·T**), and mesitylene (**1-Ag·M**) revealed a new phase (tetragonal, $I4_1/a$, $V \approx 100{,}000$ Å^3) differentiated form the guest-free phase (cubic, $I\bar{4}3d$, $V \approx 20{,}000$ Å^3) in symmetry and complexity. On the basis of X-ray data, the formulas of **1-Ag·B**, **1-Ag·T**, and **1-Ag·M** are refined as $[Ag_{30}(bpz)_{15}]\cdot 10(C_6H_6)$, $[Ag_{30}(bpz)_{15}]\cdot 9(C_7H_8)$, and $[Ag_{30}(bpz)_{15}]\cdot 8(C_9H_{12})$, respectively.

As exemplified by the structural comparison of **1-Ag** and **1-Ag·M**, the $[Ag_2(bpz)]$ network retains metal−ligand connectivity, but the cavities do not uniformly shrink or expand upon mesitylene inclusion. In **1-Ag·M**, some cavities shrink to fit a mesitylene monomer, and simultaneously others expand to fit a mesitylene dimer so that every five adjacent cavities rearrange to form a new periodic arrangement, having 8 mesitylene molecules in 5 cavities. The shortest Ag···C contacts (ca. 3.3 Å) are shorter than the sum of Van der Waals radii of Ag (1.72 Å) and C (1.70 Å)[42] but significant longer than the coordination bonds of silver−arene complexes, indicating the existence of weak Ag···π interactions between the UMC clusters and the unsaturated hydrocarbons. The unique molecular structure of the interpenetrated $[Ag_2(bpz)]$ network is responsible for this unique structural transformation. Obviously, the $Ag_3(pz)_3$ dimers have changed from staggered to slipped conformations, reflecting significant sliding between the interpenetrating networks. Nevertheless, the complicated pore size/shape rearrangement between **1-Ag** and **1-Ag·M** is not achieved by simply sliding as observed in other flexible PCPs, since sliding can only double the complexity in one dimension. Significant single-network deformation is evident by comparing the $[Ag_2(bpz)]$ networks of the cubic and tetragonal phases. Rotation freedom of the bpz ligand plays an important role in the deformation of the $[Ag_2(bpz)]$ network upon mesitylene inclusion. The bpz ligands in **1-Ag·M** possess a variety of dihedral angles (56.9−63.7°, av 60.2°), which are significantly smaller than the uniform value 67.4° presented in the guest-free framework. Additionally, the two coordinated silver centers also show certain flexibility in the bond lengths and angles. In other words, the whole $[Ag_2(bpz)]$ framework simultaneously expands, shrinks, distorts, and slides different parts of its coordination frameworks, behaving like a noncrystalline, soft material.

Considering the second-order-like phase transition behaviors of **1-Ag** during initial gas uptake, we also tried to determine the structures of the single crystals with partially loaded arene molecules. Although the shape and transparency of the single crystals do not change during the whole adsorption process, their X-ray diffraction behaviors change drastically, depending on the uptake amount. Three kinds of intermediate phases are observed from the "single crystal" diffraction patterns: (1) new single-crystal phases, (2) twinned or polycrystalline phases, and (3) amorphous-like phases. All of these intermediate states can be transformed back to the initial cubic phase by using the same "single crystal", implying that the metal−ligand connectivity retains integrity in the intermediate phases. However, the new single-crystal phases are always associated with much larger unit cells and lower symmetries compared to the guest-free cubic phase. The instability and the complexity of these single-crystalline phases baffle the diffraction data collection. The twinned or polycrystalline phases should be ascribed to the coexistence of multiple periodic domains in the same sample. The observation of amorphous-like phases indicates that in some stage of guest uptake level, the long-range order of the metal−ligand connectivity is almost destroyed by the random distribution of the guest, or the new periodic units exceed the resolution limit of the X-ray diffraction. All of these observations refer to

(42) Bondi, A. *J. Phys. Chem.* **1964**, *68*, 441.

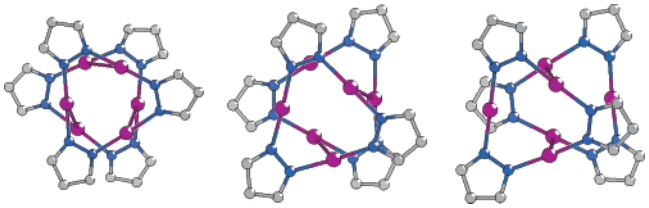

Figure 8. Three different dimer conformations of $[Ag_3(pz)_3]$ SBUs in **1-Ag-I**.

the soft nature and the existence of multiple, metastable, intermediate states of the $[Ag_2(bpz)]$ networks. It should be noted that these intermediate states are difficult to be characterized by powder X-ray diffraction techniques, which provide a sum of information on multiple crystallites in different states.

Nevertheless, one of the intermediate phases (**1-Ag·I**, tetragonal, $I\bar{4}2d$, $V \approx 60{,}000$ Å^3) provided single-crystal X-ray diffraction data, which is sufficient for the refinement of atomic positions of the $[Ag_2(bpz)]$ networks. The $[Ag_2(bpz)]$ network structure of **1-Ag·I** represents an intermediate stage of the structural transformation from **1-Ag** to **1-Ag·M**. The $Ag_3(pz)_3$ dimers of **1-Ag·I** exhibit as staggered, slipped, and partially slipped conformations, implying the energetic similarity of these molecular arrangements (Figure 8). The cavities are also disproportioned, but their sizes and shapes are similar to those of **1-Ag** (Figure S9). More interestingly, the structural comparison among **1-Ag**, **1-Ag·I**, and **1-Ag·M** demonstrates the interpenetrating $[Ag_2(bpz)]$ networks change symmetry, shape, and relative position in a complicated, nonlinear manner at different guest-uptake stages. As depicted in Figure 9, in the case of **1-Ag·I**, structural distortion (complication) mainly occurs in the *c*-axis, while for **1-Ag·M**, it mainly occurs in the *ab*-plane.

We have also measured the X-ray diffraction pattern for **1-Ag** single crystals with CO_2 inclusion. The diffraction pattern can be indexed to a very large unit cell (cubic, *I* lattice, $a = 55.583(13)$ Å, $V = 171{,}725(3)$ Å^3). Although the extremely complicated structure and the insufficient diffraction ability preclude structure solution, each $Ag_2(bpz)$ moiety can be estimated to occupy 447 Å^3 ($Z \times Z' = 48 \times 2^3$), 6.2% higher than that of **1-Ag** (421 Å^3, $Z \times Z' = 48$), corresponding to ca. 20% increase of the void volume. Therefore, the unique gas sorption isotherms of **1-Ag** can be explained by the existence of multiple metastable structures, which possess different cavities suitable for different guest aggregates. Similar conclusions are also applicable to its isomer and the Cu(I) analogue.

Coordinatively Unsaturated Metal Centers. As shown in the crystal structures of **1-Ag·B**, **1-Ag·T**, and **1-Ag·M**, the Ag_3 UMC clusters are able to form weak interactions with the aromatic rings. However, considering the comparable sizes of the cavities and the arene molecules, as well as the flexible nature of the host framework, the confinement effects should be significant. Therefore, large molecules are not suitable for examining the UMC effects of **1**. Acetylene is known to form metal$-\pi$ complexes with Ag(I) and Cu(I) with low coordination numbers. Separation of acetylene from carbon dioxide is highly demanded since they are similar in equilibrium sorption parameter and molecular size and shape.[43−46]

$[M_2(bpz)]$ shows reversible type-I isotherms for C_2H_2 and CO_2 at 273 and 298 K (Figure 10), respectively, indicating no chemical sorption process is occurring during the measurements (see Supporting Information). At room temperature, 1.0 atm, the C_2H_2 uptakes of **1-Ag** (44.1 mL/g) and **1-Cu** (57.9 mL/g) are comparable or higher than those of carbon molecular sieves (45 mL/g),[43] coordination polymer CPL-1 (42 mL/g),[44] and organic host *p-tert*-butylcalix[4]arene (18 mL/g),[45] but slightly lower than those of $Mg(HCOO)_2$ (65.7 mL/g) and $Mn(HCOO)_2$ (51.2 mL/g) formate.[46] At the same condition, the CO_2 uptakes of **1-Ag** and **1-Cu** are 30.3 and 39.1 mL/g, corresponding to C_2H_2/CO_2 uptake ratios of 1.46 and 1.48, respectively. On the other hand, isomers **2** can adsorb less C_2H_2 and exhibit lower C_2H_2/CO_2 uptake ratios (Table 4).

The C_2H_2/CO_2 uptake ratio can be used to estimate the relative affinity of C_2H_2 and CO_2 toward the pore surface. Carbon molecular sieves (1.25) and *p-tert*-butylcalix[4]arene (1.25) have low C_2H_2/CO_2 uptake ratios, since their pore surfaces cannot distinguish between the similar gas molecules. Higher C_2H_2/CO_2 uptake ratios are observed for $Mn(HCOO)_2$ (1.34) and $Mg(HCOO)_2$ (1.47), which contain hydrogen-bond-accepting carbonyl oxygen atoms on the pore surfaces. The uncoordinated carbonyl groups of CPL-1 are suitable to form strong hydrogen bonds to C_2H_2, thus giving a very high C_2H_2/CO_2 uptake ratio.

The isosteric heats of C_2H_2 and CO_2 were estimated by the Clausius−Clapeyron equation (273 and 298 K). In general, the isosteric heat of C_2H_2 for the individual compound is higher than that of CO_2. The four-fold interpenetrated isomers **1** exhibit substantially large isosteric heat difference between C_2H_2 and CO_2. In contrast, the isosteric heat difference between C_2H_2 and CO_2 are very small for the eight-fold interpenetrated isomers **2**. Regarding the electronegativity of the framework components, the hydrogen-bonding ability of the pore surface of $[M_2(bpz)]$ is much weaker than that of metal carboxylate. Comparing the structures of the pore surfaces of **1** and **2**, the narrower cavity and less accessible UMC give rise to the higher contribution from the confinement effect and the lower contribution from the metal$\cdots\pi$ interaction, thus decreasing the C_2H_2/CO_2 selectivity and isosteric heat difference. Enlightened by the crystal structures of arene inclusion complexes of **1-Ag**, we concluded that the weak metal$\cdots\pi$ interactions formed between UMC clusters and C_2H_2 molecules should be responsible for the discrimination effect of C_2H_2 from CO_2.

One may notice that the isosteric heats of C_2H_2 for the four-fold interpenetrated isomers **1** are exceptionally low. The isosteric heat of C_2H_2 for **1-Ag** are substantially lower than those for CPL-1 (42.5 kJ/mol), $Mg(HCOO)_2$ and $Mn(HCOO)_2$ (38.5 kJ/mol),[46] and even lower than that for **2-Ag**. It should be noted that the measured isosteric heat contains not only the host−guest binding energy but also the structural transformation energy. First-principle calculation has demonstrated the slight distortion of CPL-1 consumes 6.9 kJ/mol upon C_2H_2 adsorption. The isosteric heats of C_2H_2 for magnesium and manganese formats are relatively high because the adsorption does not induce structural transformation, although only very weak hydrogen bonding is observed between the C_2H_2 and the pore

(43) Reid, C. R.; Thomas, K. M. *Langmuir* **1999**, *15*, 3206−3218.
(44) Matsuda, R.; Kitaura, R.; Kitagawa, S.; Kubota, Y.; Belosludov, R. V.; Kobayashi, T. C.; Sakamoto, H.; Chiba, T.; Takata, M.; Kawazoe, Y.; Mita, Y. *Nature* **2005**, *436*, 238−241.
(45) Thallapally, P. K.; Dobrzańska, L.; Gingrich, T. R.; Wirsig, T. B.; Barbour, L. J.; Atwood, J. L. *Angew. Chem., Int. Ed.* **2006**, *45*, 6506−6509.
(46) Samsonenko, D. G.; Kim, H.; Sun, Y.; Kim, G.-H.; Lee, H.-S.; Kim, K. *Chem. Asian J.* **2007**, *2*, 484−488.

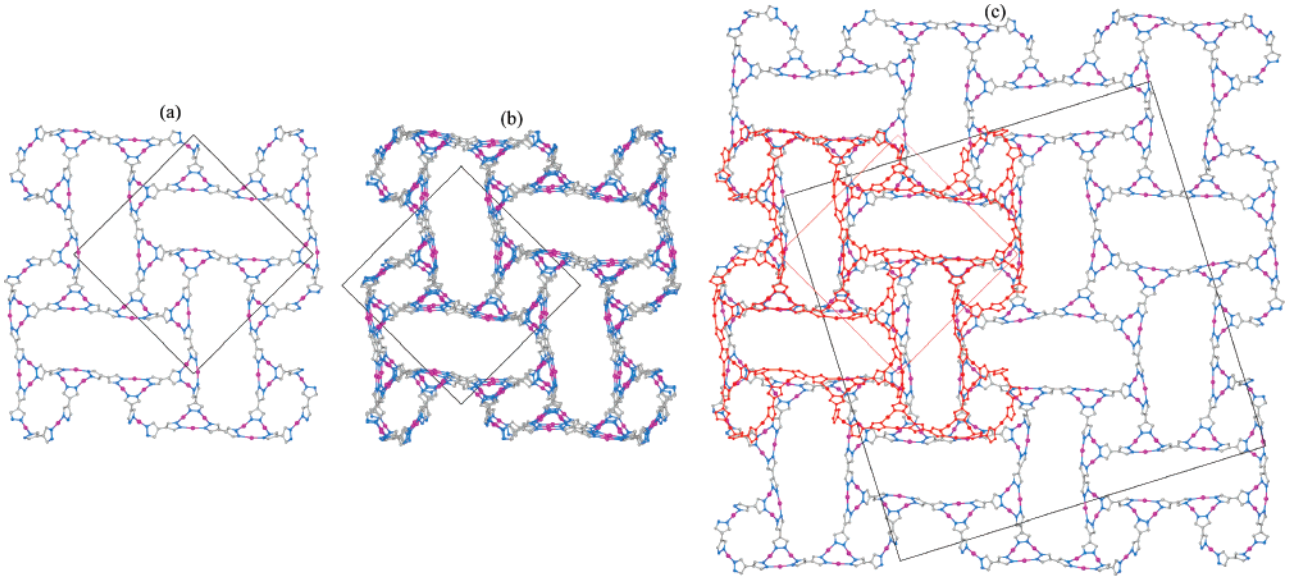

Figure 9. Parallel projection of a single [Ag_2(bpz)] network of **1-Ag** (a), **1-Ag-I** (b), and **1-Ag·M** (c) along the crystallography four-fold symmetry axis. A [Ag_2(bpz)] network of **1-Ag** (red) is superimposed on that of **1-Ag·M** to highlight the structural deformation.

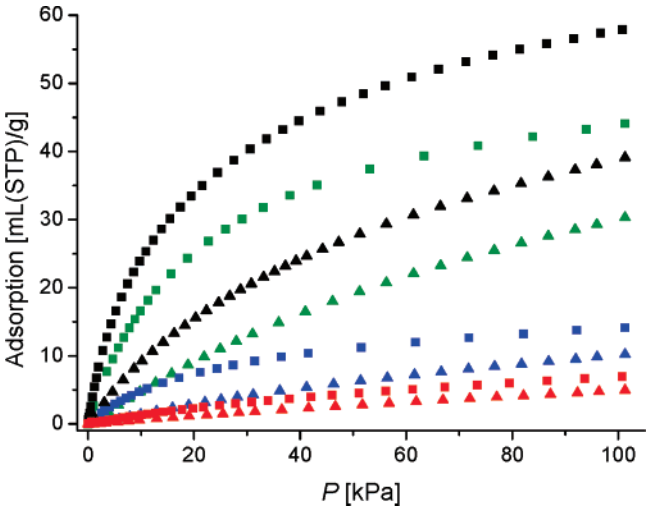

Figure 10. C_2H_2 (square) and CO_2 (triangle) adsorption isotherms of **1-Ag** (green), **1-Cu** (black), **2-Ag** (blue), and **2-Cu** (red) at 298 K.

Table 4. C_2H_2/CO_2 Separation Parameters of [M_2(bpz)] Isomers

	1-Ag	1-Cu	2-Ag	2-Cu
C_2H_2 uptake[a] [mL/g]	44.1	57.9	14.1	6.9
CO_2 uptake[a] [mL/g]	30.3	39.1	10.2	5.0
C_2H_2/CO_2 uptake ratio[a]	1.46	1.48	1.38	1.38
$\Delta H(C_2H_2)$[b] [kJ/mol]	28.4	32.0	33.2	32.0
$\Delta H(CO_2)$[b] [kJ/mol]	19.5	27.5	30.3	30.2
$\Delta H(C_2H_2) - \Delta H(CO_2)$ [kJ/mol]	8.9	4.5	2.9	1.8

[a] Adsorption amount at 298 K, 1.0 atm. [b] Calculated from fractional coverage 0.1 mol/g at 273 and 298 K using Clausius−Clapeyron equation.

surfaces. We have shown that the atomic positions of **1-Ag** can potentially move more than 3 Å upon guest inclusion (Figure 9). On the other hand, the potential atomic movements for **2-Ag** should be very small due to the highly interpenetrated networks, low porosity, and low flexibility. Therefore, the absolute adsorption isosteric heats of a given gas for [M_2(bpz)] represent relative flexibility rather than the gas binding energy of the host framework.

Conclusions

The coinage metal bipyrazolate [M_2(bpz)] is an intrinsic supramolecular isomerism system, though the coordination geometries of the metal ions and the organic ligands are predictable. Four metal organic frameworks, based on two basic structural types (isomers **1** and **2**) and two similar coinage metals (Ag and Cu), are selectively synthesized by precise control of the reaction conditions. The interesting crystallization behaviors of these isomers demonstrate the importance of kinetic factors in this low-solubility system, arising from the strong metal−pyrazolate coordination bonds and the polymeric nature of [M_2(bpz)]. Despite four- and eight-fold interpenetration of the coordination networks, [M_2(bpz)] isomers still contain extra frameworks. The combination of high stability and UMCs in the porous [M_2(bpz)] frameworks, in particular in the highly porous four-fold interpenetrated isomer **1**, are remarkable since Ag(I)/Cu(I) species are usually very unstable and not suitable for the construction of porous coordination polymers.

[M_2(bpz)] can adsorb different guest molecules with molecular sizes larger than the pore apertures, reflecting the framework flexibilities of these highly interpenetrated networks. Excess adsorption and unusual adsorption isotherms are also observed for some of these compounds. Depending on the structural types and metal ions, the extent of framework flexibilities varies in these compounds with a general trend that four-fold interpenetration is greater than eight-fold interpenetration and Ag > Cu. Importantly, the [M_2(bpz)] crystals retain single-crystallinity during guest uptake/release. Single-crystal diffraction studies on **1-Ag** revealed that the structural transformations are carried out in a complicated way rather than simply expanding, shrinking, or sliding the whole framework. In response to different guest-uptake levels, the coordination framework rearranges its pore size and shape nonuniformly to fit different guest oligomers. Moreover, single-crystal diffraction studies of the intermediate structures (partial guest loading) illustrated that the structural transformation does not monotonously change with increase of guest loading as generally believed for flexible PCPs. Finally, the UMC clusters are demonstrated to facilitate the

accommodation of unsaturated hydrocarbons such as benzene, toluene, mesitylene, and acetylene via weak metal$\cdots\pi$ interactions.

In summary, we have demonstrated that not only Ag(I) but also Cu(I) can be immobilized as a guest-accessible, soft Lewis acid site in a PCP with a large cavity. The guest sorption and single-crystal diffraction studies revealed that these metal bipyrazolates are much softer than other crystalline materials.

Acknowledgment. This work was supported by a Grants-in-Aid for Scientific Research in a Priority Area "Chemistry of Coordination Space" (#434) and Core Research for Evolutional Science and Technology (CREST) from the Ministry of Education, Culture, Sports, Science and Technology, Government of Japan. J.-P.Z. is grateful to JSPS for a postdoctoral fellowship.

Supporting Information Available: Crystallographic data in CIF format; additional plots and powder XRD and TG data. This material is available free of charge via the Internet at http://pubs.acs.org.

JA075408B